Journal of Aeronautics, Astronautics and Aviation, Vol. 51, No. 2, pp. 201 – 212 (2019)
DOI: 10.6125/JoAAA.201906_51(2).05

Effect of Skin and Spar Laminate Orientations on Flutter of Composite UAV Wing *

Nurul-Zubaidah Zaki **, Fareed A. Mazaha, Ainullotfi Abdul-Latif, Shuhaimi Mansor, Mastura Ab Wahid, Md. Nizam Dahalan, Norazila Othman, Shabudin B. Mat, and Mohd Nazri Mohd Nasir

Aeronautics Laboratory, School of Mechanical Engineering, Faculty of Engineering, Universiti Teknologi Malaysia, 81310 UTM Skudai, Johor, Malaysia.

ABSTRACT

This paper presents an analytical study on the optimisation of composite laminate orientation lay-up to achieve the maximum flutter with minimum weight penalty. The study is carried out by using UTM CAMAR UAV swept back wing as a case study where the wing consists of two spars located at 35% and 55% of the wing chord length. The laminate lay-up of the spar and the wing skin are optimised by considering different variations of laminate ply orientation while the number of plies for each part are set to be constant throughout the work. The finite element analysis software, Abaqus, was used to obtain the structural natural frequencies for bending and torsion modes. The bending stiffness, torsion stiffness and the eigenvalues of the aeroelasticity equation of motion are computed using the mathematical software, MATLAB. The maximum flutter speed obtained from the study is 238.93 m/s with laminate configuration at [45°/-45°/45°/-45°] for wing skin, [45°/-45°/45°] for forward spar, [45°/-45°]s for aft spar and [0°/0°/0°/0°] for the wing tip.

Keywords: Flutter speed, Composite wing, Dynamic aeroelasticity, Composite laminates, Fibre orientation

I. INTRODUCTION

Flutter is the product of interaction between elastic, aerodynamic and inertial forces and is associated with two or more modes of motion such as bending and torsion, and can cause catastrophic failure [1]. This phenomenon usually occur on structures with high aerodynamic loadings such as wings, tails and control surfaces. The critical flutter speed is one of the important parameters that need to be considered in aircraft designing process as the oscillations of the undamped vibrations may be amplified beyond the critical speed. One of the factors influencing flutter speed is structural stiffness which is influenced by the structural shape, design and materials [2].

For the past 40 years, researchers have been trying to investigate and study composite materials application in the aircraft structure due to its high specific strength to weight ratio. The material also offers a great advantage to tackle dynamic and aeroelastic problems such as flutter and divergence [3-7]. Composite material stiffness and strength can be tailored by altering the fibre orientations and number of laminate plies [8-10]. Also, properties such as laminate fibre orientations and elastic modulus ratio have significant effects on the limit cycle oscillation and flutter speed [1].

In the case of real aircraft wings, the structures are usually composed of internal components such as ribs, spars, stringers and frames which act as stiffeners for the wing skin. Wing spars can be altered in order to control aeroelastic behaviours such as bending and torsion deflections [11]. According to Zaki [1], the location of spar in the wing gives a significant effect on the flutter speed and bending stiffness. In the study, the maximum flutter speed is achieved when the front and the rear spars are located at 0.35 and 0.55 of chord length respectively for the swept-back composite wing.

* Manuscript received, February 1, 2018, final revision, April 15, 2019.
** To whom correspondence should be addressed, E-mail: nzubaidah2@live.utm.my

II. PROBLEM MODELLING

In this study, the UTM CAMAR UAV swept-back composite wing are applied as the case study in which the full model is as shown in Figure 1 and the simplified cantilever swept-back wing is shown in Figure 2. The composite material that was used in the study is carbon fibre-epoxy with the parameters shown in Table 1. Meanwhile, the parameters of the cantilevered swept-back wing is shown in Table 2.

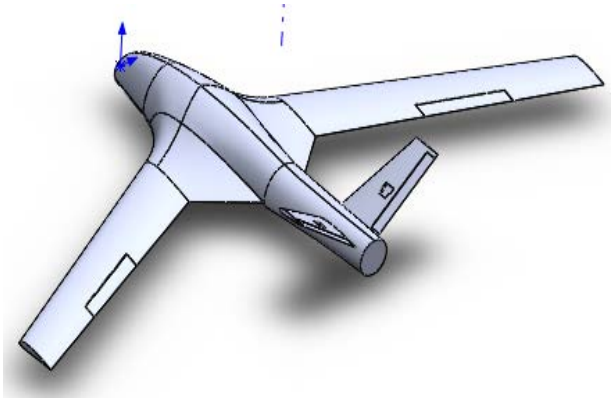

Figure 1 UTM CAMAR UAV model

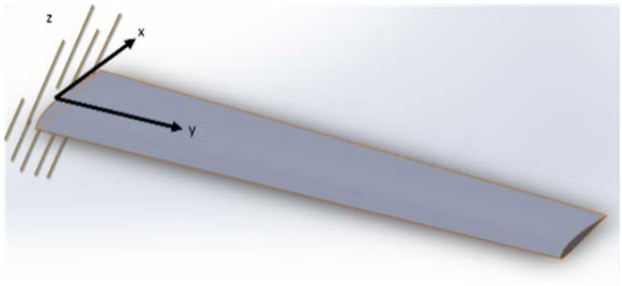

Figure 2 Simplified wing model

Table 1 Carbon fibre-epoxy composites mechanical properties

Parameter	Value
Young's modulus (E_1, E_2), GPa	70
Shear modulus (G_{12}), GPa	5
Poisson's ratio (ν)	0.1
Density (ρ), kg/m^3	1600

Table 2 UTM CAMAR UAV wing parameters

Parameter	Value
Semi-span (s), m	1.5
Chord, m	0.222
Flexural axis from nose, x_f	0.48c
Centre of mass from nose, m	0.50c
Heave stiffness, K_k	$(2\pi\omega_k)^2$
Pitch stiffness, K_θ	$(2\pi\omega_\theta)^2$
Lift curve slope	6.51113
Air density (kg/m^3)	1.225
Sweep Angle	25°
Aerofoil	SD7062

The binary aeroelastic equation of motion are applied in order to obtain the flutter velocity of the composite wing for different composite laminate orientation. The equation of motion are derived by assuming there are two different spring attached to the flexural axis of the straight thin wing as shown in Figure 3.

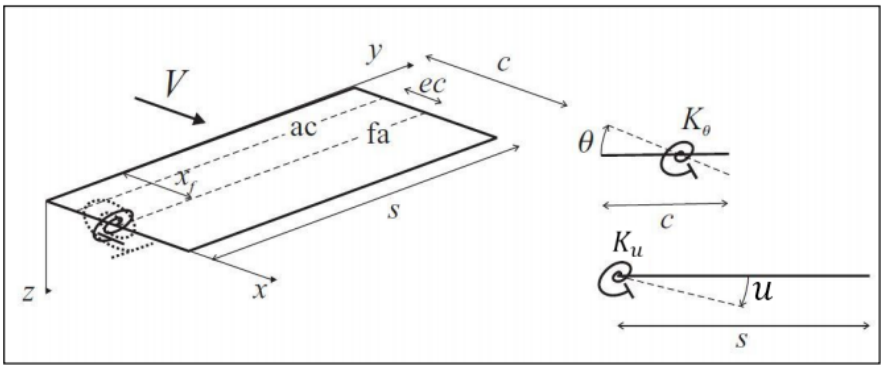

Figure 3 Binary aeroelastic model

The wing model as shown in Figure 3 are assumed to have a uniform mass distribution with the mass axis on the mid-chord of the wing [Wright & Cooper (2008)]. The equations of motion for the wing, without considering the aerodynamic forces such as aerodynamic damping and stiffness is:

$$\begin{bmatrix} \frac{ms^3c}{3} & \frac{ms^2}{2}\left(\frac{c^2}{2}-cx_f\right) \\ \frac{ms^2}{2}\left(\frac{c^2}{2}-cx_f\right) & ms\left(\frac{c^3}{3}-c^2x_f+cx_f^2\right) \end{bmatrix}\begin{Bmatrix}\ddot{u}\\ \ddot{\theta}\end{Bmatrix}+\begin{bmatrix}K_u & 0\\ 0 & K_\theta\end{bmatrix}\begin{Bmatrix}u\\ \theta\end{Bmatrix}=\begin{Bmatrix}0\\0\end{Bmatrix} \quad (1)$$

Where, the inertia matrix of the equation is:

$$\begin{bmatrix} I_u & I_{u\theta} \\ I_{u\theta} & I_\theta \end{bmatrix}=\begin{bmatrix} \frac{ms^3c}{3} & \frac{ms^2}{2}\left(\frac{c^2}{2}-cx_f\right) \\ \frac{ms^2}{2}\left(\frac{c^2}{2}-cx_f\right) & ms\left(\frac{c^3}{3}-c^2x_f+cx_f^2\right) \end{bmatrix} \quad (2)$$

Assuming there are no inertial coupling, the bending and torsional natural frequencies are:

$$\omega_u=\sqrt{\frac{K_u}{I_u}}\ ,\omega_\theta=\sqrt{\frac{K_\theta}{I_\theta}} \quad (3)$$

By considering the strip theory, the derivation of the aerodynamic forces is:

$$dL=\frac{1}{2}\rho V^2c\ dy\ a_w\left(\frac{y\dot{\kappa}}{V}+\theta\right) \quad (4)$$

$$dM=\frac{1}{2}\rho V^2c^2dy\ \left[ea_w\left(\frac{y\dot{\kappa}}{V}+\theta\right)+M_{\dot{\theta}}\left(\frac{\dot{\theta}c}{4V}\right)\right. \quad (5)$$

The generalized aerodynamic forces are [Wright & Cooper (2008)]:

$$Q_k=\frac{\partial(\delta W)}{\partial(\delta_u)}=-\int_0^s ydL=\frac{1}{2}\rho V^2cs^2a_w\left(\frac{\dot{\kappa}s}{3V}+\frac{\theta}{2}\right) \quad (6)$$

$$Q_\theta=\frac{\partial(\delta W)}{\partial(\delta_\theta)}=\int_0^s dM=\frac{1}{2}\rho V^2c^2s[ea_w\left(\frac{\dot{\kappa}s}{2V}+\theta\right)+M_{\dot{\theta}}\frac{\dot{\theta}c}{4V} \quad (7)$$

Therefore, the full aeroelastic equation of motion are:

$$\begin{bmatrix} I_u & I_{u\theta} \\ I_{u\theta} & I_\theta \end{bmatrix}\begin{Bmatrix}\ddot{u}\\ \ddot{\theta}\end{Bmatrix}+\rho V\begin{bmatrix} \frac{cs^2a_w}{6} & 0 \\ -\frac{ec^2s^2a_w}{4} & -\frac{c^3s}{8}M_{\dot{\theta}} \end{bmatrix}\begin{Bmatrix}\dot{u}\\ \dot{\theta}\end{Bmatrix}+\left\{\rho V^2\begin{bmatrix} 0 & \frac{cs^2a_w}{4} \\ 0 & -\frac{ec^2sa_w}{2} \end{bmatrix}+\begin{bmatrix}K_u & 0\\ 0 & K_\theta\end{bmatrix}\right\}\begin{Bmatrix}u\\ \theta\end{Bmatrix}=\begin{Bmatrix}0\\0\end{Bmatrix} \quad (8)$$

Or, can be written as:

$$\mathbf{A}\ddot{q}+(\rho V\mathbf{B}+\mathbf{D})\dot{q}+(\rho V^2\mathbf{C}+\mathbf{E})q=0 \quad (9)$$

$\boldsymbol{A}, \boldsymbol{B}, \boldsymbol{C}, \boldsymbol{D}, \boldsymbol{E}$ are the structural inertia, aerodynamic damping, aerodynamic stiffness, structural damping and structural stiffness matrices, respectively.

III. METHODOLOGY

The stiffness of the wing is varied by applying different ply orientations for composite laminates on the wing. Parameters of stiffness that are analysed in this project are bending stiffness, K_u, and torsional stiffness, K_θ. Different composite ply orientations on different parts of the wing results in different stiffness of the wing, subsequently affecting the flutter speed of the wing. Stiffness of the wing is represented using the value of natural frequency extracted for the wing model using the finite element software, Abaqus. The wing internal structures consist of two spars located at 35% and 55% of the wing chord as shown in Figure 4 and Table 2.

The first type of analysis was done by fixing the composite ply orientations on the spars while those for the wing skin were varied. The second one was done by fixing the wing skin composite ply orientations but varying those for the wing spars. The configurations giving the best results from these two types of analysis were then combined for further analysis.

Table 3 Spar position along the chord length

Spar Position	%C	Distance from Leading Edge (LE) (mm)	
		Wing Inboard	Wing Outboard
7	35	93.41	67.69
11	55	146.79	106.37

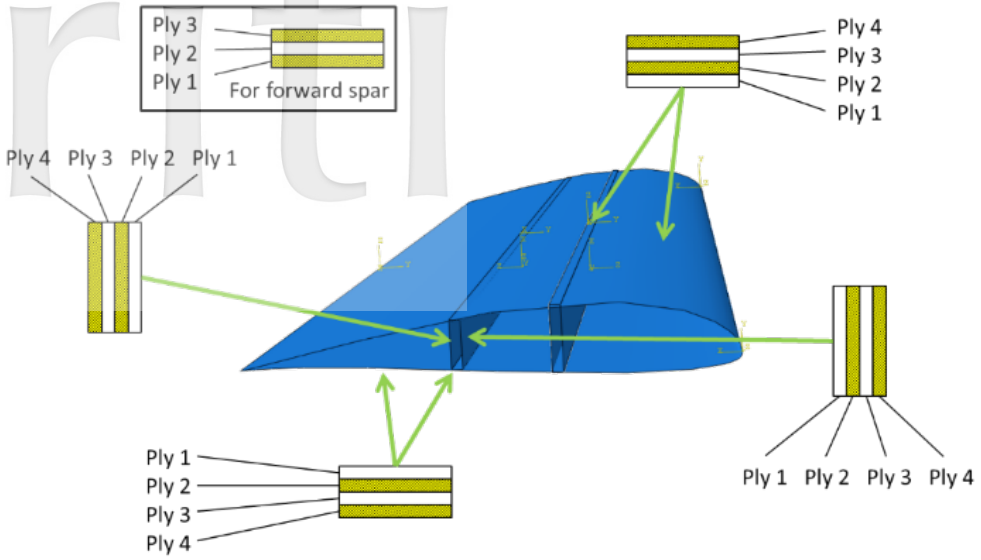

Figure 4 Ply stack on each surface of the parts

IV. RESULTS

4.1 Fixed spar orientation case

The analysis of flutter on a composite UAV wing with different composite laminate orientation was done by fixing the spars composite laminate orientation at 0°. The laminate orientation of the wing skin which is assigned as top and bottom skin are changed from -90° to 90° with 4 laminate plies. The bending and torsion natural frequencies were obtained from the finite element analysis and the flutter velocity was calculated and shown in Table 3. The results of the flutter speed and the frequencies with variations of laminate orientation are plotted in Figure 5 and Figure 6.

Table 3 Frequencies and flutter speeds for varying skin ply orientations (fixed spar)

Laminate ply orientation		Frequency (Hz)		$V_{flutter}$ (m/s)
Top skin	Bottom skin	Bending	Torsion	
$[-90°]_4$	$[-90°]_4$	16.445	123.65	136.93
$[-75°]_4$	$[-75°]_4$	18.972	129.42	142.55
$[-60°]_4$	$[-60°]_4$	23.511	141.50	154.69
$[-45°]_4$	$[-45°]_4$	26.452	139.23	150.53
$[-30°]_4$	$[-30°]_4$	26.382	133.97	144.38
$[-15°]_4$	$[-15°]_4$	24.022	123.68	133.46
$[0°]_4$	$[0°]_4$	21.829	122.46	133.10
$[15°]_4$	$[15°]_4$	21.900	126.94	138.31
$[30°]_4$	$[30°]_4$	22.106	140.54	154.12
$[45°]_4$	$[45°]_4$	22.462	154.60	170.38
$[60°]_4$	$[60°]_4$	23.180	159.20	175.43
$[75°]_4$	$[75°]_4$	24.734	145.04	158.17
$[90°]_4$	$[90°]_4$	26.863	123.21	131.54

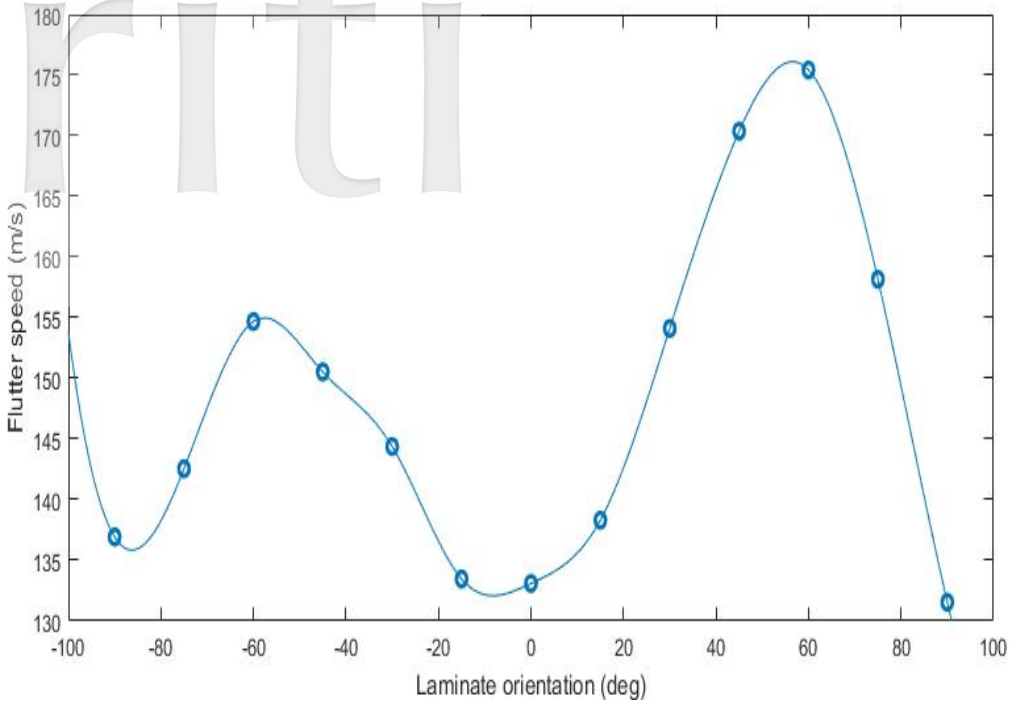

Figure 5 Flutter speeds for varying skin ply orientations (fixed spar)

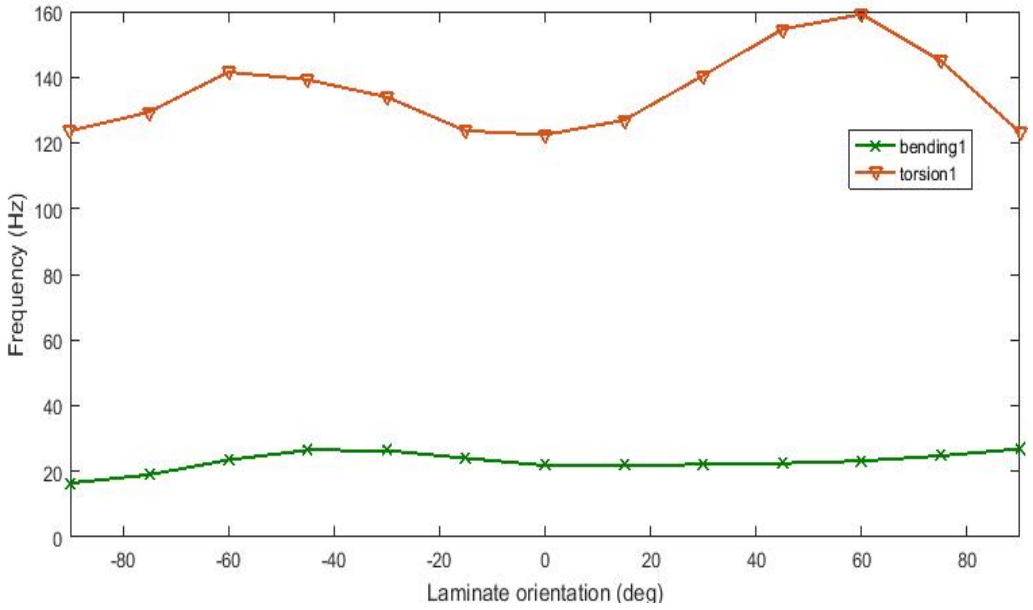

Figure 6 Bending and torsion mode frequencies for varying skin ply orientations (fixed spar)

4.2 Mixed skin ply orientation for fixed spar case

The effect of ply orientation on the flutter speed can be further observed by looking into different cases of ply orientation combinations for the skin laminate. Tables 4a, 4b and 4c give the results for three different combination cases A, B and C representing symmetrical, anti-symmetrical with alternate orientations, and anti-symmetrical with double alternate orientations composite lay-ups, respectively. The flutter speeds resulting are plotted in Figure 7 with 4 different variations for each case.

Table 4a Flutter speeds and frequencies for Case A

No	Ply Orientation		Frequency (Hz)		$V_{flutter}$ (m/s)
	Top Skin	Bottom Skin	Bending	Torsion	
1	$[-45°/45°]_s$		23.359	194.770	216.770
2	$[45°/-45°]_s$		23.359	194.700	216.680
3	$[-45°/45°]_s$	$[45°/-45°]_s$	23.359	194.740	216.730
4	$[45°/-45°]_s$	$[-45°/45°]_s$	23.359	194.730	216.720

Table 4b Flutter speeds and frequencies for Case B

No	Ply Orientation		Frequency (Hz)		$V_{flutter}$ (m/s)
	Top Skin	Bottom Skin	Bending	Torsion	
1	$[-45°_2/45°_2]_2$		23.351	193.790	215.630
2	$[45°_2/-45°_2]_2$		23.361	194.800	216.800
3	$[-45°_2/45°_2]_2$	$[45°_2/-45°_2]_2$	23.358	194.450	216.390
4	$[45°_2/-45°_2]_2$	$[-45°_2/45°_2]_2$	23.355	194.480	216.430

Table 4c Flutter speeds and frequencies for Case C

No	Ply Orientation		Frequency (Hz)		$V_{flutter}$ (m/s)
	Top Skin	Bottom Skin	Bending	Torsion	
1	$[-45°_2/45°_2]$		23.333	191.200	212.630
2	$[45°_2/-45°_2]$		23.353	193.370	215.140
3	$[-45°_2/45°_2]$	$[45°_2/-45°_2]$	23.347	193.430	215.210
4	$[45°_2/-45°_2]$	$[-45°_2/45°_2]$	23.342	193.440	215.230

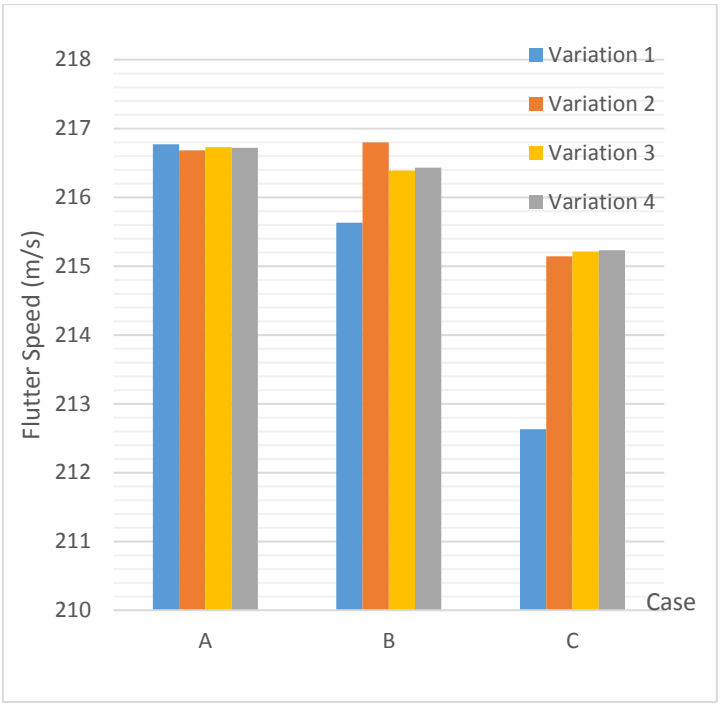

Figure 7 Flutter speeds at different cases of skin laminate ply orientation combinations (fixed spar)

4.3 Fixed skin orientation case

For the next analysis, the ply orientations were fixed for both the top and the bottom skins at 0°, while the orientations on the spar were varied from -90° to 90°. The number of laminate plies for the front spar (at 35% chord) and rear spar (at 55% chord) are 3 and 4, respectively.

Table 5 Frequencies and flutter speeds for varying spar ply orientations (fixed skin)

Laminate ply orientation		Frequency (Hz)		$V_{flutter}$ (m/s)
Front spar	Rear spar	Bending	Torsion	
$[-90°]_3$	$[-90°]_4$	16.445	123.65	136.93
$[-75°]_3$	$[-75°]_4$	18.972	129.42	142.55
$[-60°]_3$	$[-60°]_4$	23.511	141.58	154.69
$[-45°]_3$	$[-45°]_4$	26.452	139.23	150.53
$[-30°]_3$	$[-30°]_4$	26.382	133.97	144.38
$[-15°]_3$	$[-15°]_4$	24.022	123.68	133.46
$[0°]_3$	$[0°]_4$	21.829	122.46	133.10
$[15°]_3$	$[15°]_4$	22.053	127.77	139.21
$[30°]_3$	$[30°]_4$	23.832	140.46	153.23
$[45°]_3$	$[45°]_4$	24.441	146.16	159.62
$[60°]_3$	$[60°]_4$	22.363	140.08	153.47
$[75°]_3$	$[75°]_4$	18.539	129.35	142.66
$[90°]_3$	$[90°]_4$	16.445	123.65	136.93

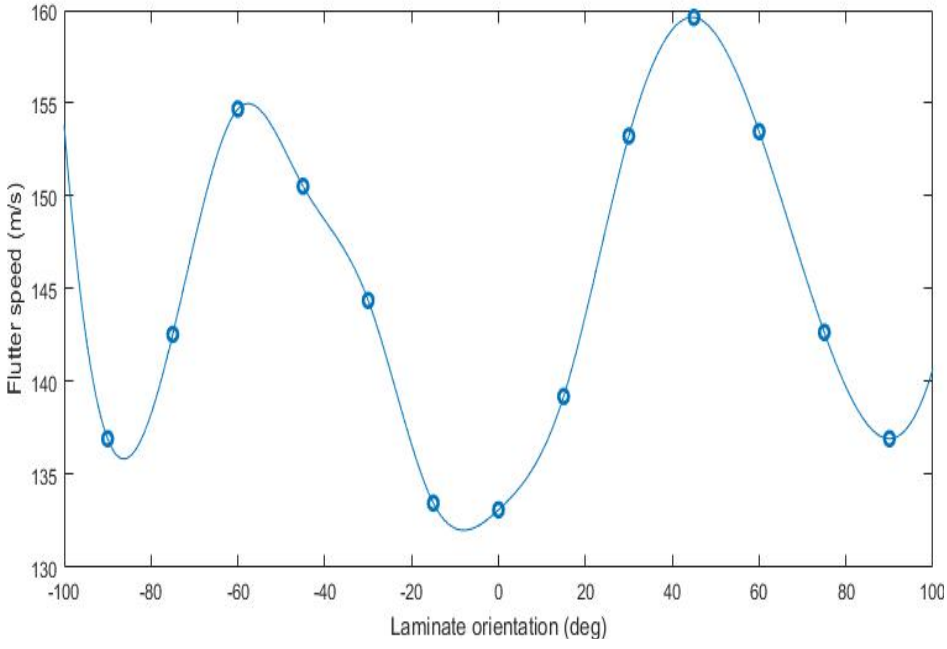

Figure 8 Flutter speeds for varying spar ply orientations (fixed skin)

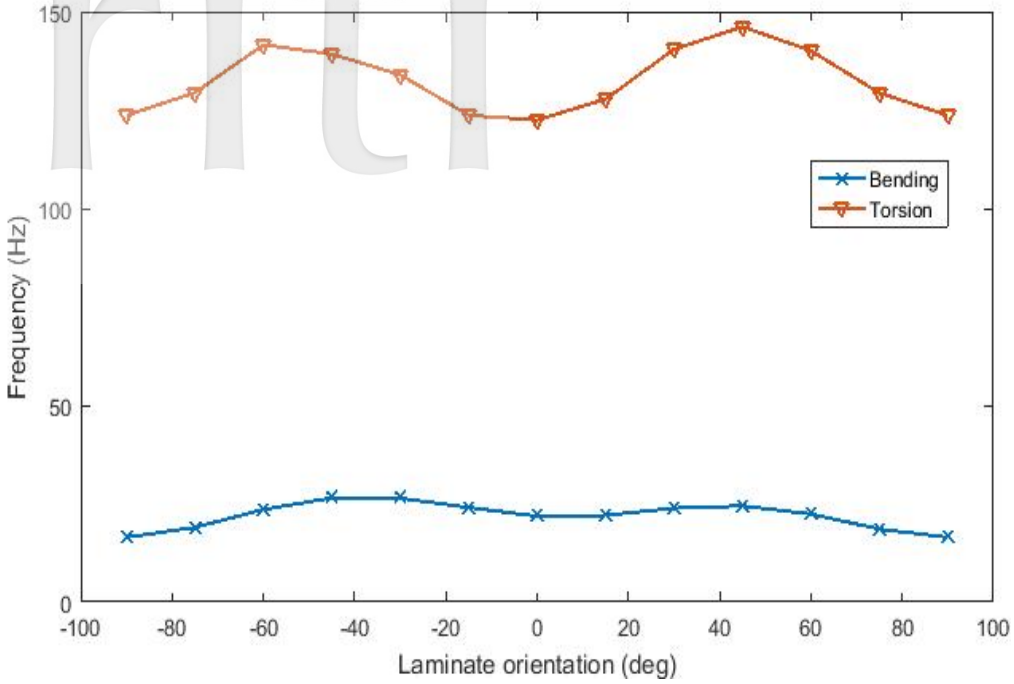

Figure 9 Bending and torsion mode frequencies for varying spar ply orientations (fixed skin)

4.4 Mixed spar ply orientation for fixed skin case

The analysis of flutter can be further extended by combining different composite laminate orientation configurations for the front and the rear spars. The different variations of laminates are categorized as Cases P, Q, R, and S, with the respective configurations for each of the cases as shown in Table 6.

From the results in Figure 10, all cases are showing almost the same values of flutter speed, between 159.96 m/s to 161.53 m/s i.e. within 0.98% range. In general, these cases of P, Q, R and S give higher values of flutter speeds compared to constant angle ply combinations as shown in Table 5 earlier. The results also show that having different orientations between flange and web of the spar do not affect the flutter speed much.

Table 6 Flutter speeds and frequencies for different spar orientation configurations (skin fixed)
**f,w is flange and web, respectively*

Case	Ply Orientation		Frequency (Hz)		$V_{flutter}$ (m/s)
	Forward Spar	Aft Spar	Bending	Torsion	
1	$[-45°/45°/-45°]$	$[-45°/45°]_s$	27.079	147.520	159.960
2	$[45°/-45°/45°]$	$[45°/-45°]_s$	24.501	148.390	162.200
3	$[-45°/45°/-45°]$ f $[45°/-45°/45°]$ w	$[-45°/45°]_s$ f $[45°/-45°]_s$ w	24.481	147.810	161.530
4	$[45°/-45°/45°]$ f $[-45°/45°/-45°]$ w	$[45°/-45°]_s$ f $[-45°_2/45°_2]$ w	27.091	148.320	160.890

4.5 Combination of Skin and Spar Cases

All these four cases (P, Q, R, S) with varying spar configurations were next combined with different wing skin orientation cases (A, B, C) earlier to find a pair that giving the highest flutter speed. The results for flutter speeds, bending natural frequencies and torsional natural frequencies for the various combinations of cases are presented in Tables 7, 8, 9 and 10. The flutter speeds for all the combinations are plotted in Figure 11.

Table 7 Results for combination of cases (Case P for the spars)

Plies Orientation Case		Frequency (*Hz*)		$V_{flutter}$ (*m/s*)
Skin	Spar	Bending	Torsion	
A-1	P	28.163	214.760	238.00
A-2	P	28.163	214.680	237.91
A-3	P	28.163	214.730	237.97
A-4	P	28.163	214.710	237.94
B-1	P	28.156	213.670	236.74
B-2	P	28.162	214.960	238.23
B-3	P	28.161	214.450	237.64
B-4	P	28.158	214.980	238.26
C-1	P	28.136	210.860	233.47
C-2	P	28.148	213.990	237.11
C-3	P	28.145	213.460	236.50
C-4	P	28.139	213.450	236.49

Table 8 Results for combination of cases (Case Q for the spar)

Plies Orientation Case		Frequency (*Hz*)		$V_{flutter}$ (*m/s*)
Skin	Spar	Bending	Torsion	
A-1	Q	25.664	214.330	238.55
A-2	Q	25.664	214.240	238.45
A-3	Q	25.664	214.300	238.52
A-4	Q	25.664	214.280	238.49
B-1	Q	25.658	213.150	237.18
B-2	Q	25.663	214.650	238.93
B-3	Q	25.661	214.000	238.17
B-4	Q	25.661	214.100	238.29
C-1	Q	25.641	210.440	234.04
C-2	Q	25.652	213.910	238.07
C-3	Q	25.648	213.040	237.06
C-4	Q	25.646	213.330	237.40

Table 10 Results for combination of cases (Case S for the spar)

Plies Orientation Case		Frequency (*Hz*)		$V_{flutter}$ (*m/s*)
Skin	Spar	Bending	Torsion	
A-1	S	28.166	214.880	238.14
A-2	S	28.166	214.790	238.04
A-3	S	28.166	214.850	238.10
A-4	S	28.167	214.820	238.07
B-1	S	28.159	213.680	236.75
B-2	S	28.167	215.180	238.49
B-3	S	28.164	214.560	237.77
B-4	S	28.161	214.610	237.83
C-1	S	28.137	210.790	233.39
C-2	S	28.153	214.320	237.49
C-3	S	28.148	213.560	236.61
C-4	S	28.142	213.600	236.66

From the results in Figure 11, the combination giving the highest flutter speed is Case B, lay-up pattern number 2 for the skin, with case Q for the spar. The configuration of ply orientations for this case is as in Table 11. From Table 11, the laminate ply orientations for each part are applied to the final wing design undergoing final computation of flutter speed, giving a result of 238.93 m/s.

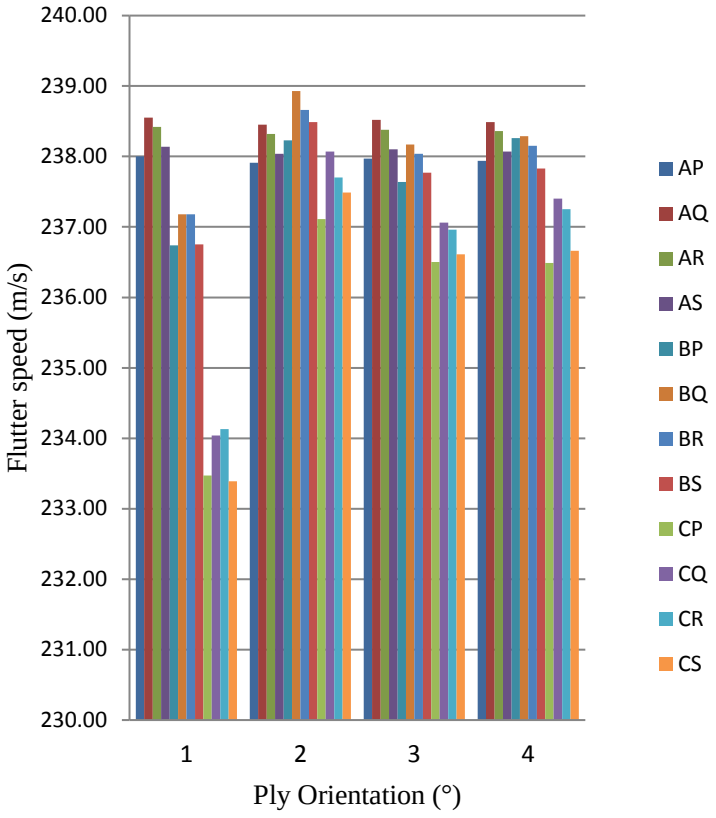

Figure 11 Result for flutter speed of combination of cases.

Table 11 Final plies orientation configuration of wing parts.

Wing Parts	Plies Orientation
Skin	$[45°/-45°]_2$
Forward Spar	[45°/-45°/45°]
Aft Spar	$[45°/-45°]_s$
Wing Tip	[0°/0°/0°/0°]

4.6 Observed trends

The analysis of the flutter speed is governed by the aeroelastic equations of motion derived from the binary wing model. From the analysis done, torsional stiffness is shown to give higher impact to the value of flutter speed compared to bending stiffness. Bending stiffness may affect the flutter speed by small value but it is shown to be not significant. Therefore, it is important for a structure to have high torsional stiffness to get a high value of flutter speed. From the results, the value used that differ the flutter speed value is the natural frequency of the structure, which is for bending motion and torsional motion in this case. Since the natural frequency is directly proportional to the stiffness of a structure, the value of natural frequency is taken to be affecting the flutter speed as well to replace the stiffness terms.

V. CONCLUSIONS

From this study, the ply orientation configuration for the wing skin and the spars of the wing of UTM CAMAR UAV giving highest flutter speed was determined. The results of the plies orientation are [45°/-45°]2 for wing skin, [45°/-45°/45°] for forward spar, $[45°/-45°]_s$ for aft spar and [0°/0°/0°/0°] for the wing tip. The highest flutter speed obtained from this combination is 238.93 m/s.

REFERENCES

[1] Zaki, NZ, Study of Flutter on a Composite UAV Wing, in Faculty of Mechanical Engineering. 2017, Universiti Teknologi Malaysia.

[2] Jin P, Zhong X, Flutter characteristic study of composite sandwich panel with functionally graded foam core. International Journal of Aerospace Engineering, 2016.

[3] Guo SJ, Banerjee JR, Cheung CW, "The effect of laminate lay-up on the flutter speed of composite wings," *Journal of Aerospace Engineering*, Vol. 217, No. 3, 2003, pp. 115-122.

[4] Yao G, Li FM, "Chaotic motion of a composite laminated plate with geometric nonlinearity in subsonic flow," *International Journal of Non-Linear Mechanics*, Vol. 50, 2013, pp. 81-90.

[5] Zhao H, Cao D, "A study on the aero-elastic flutter of stiffened laminated composite panel in the supersonic flow," *Journal of Sound and Vibration*, Vol. 332, No. 19, 2013, pp. 4668-4679.

[6] Stodieck O, Cooper JE, Weaver PM, Kelly P, "Improved aeroelastic tailoring using tow-steered composites," *Composite Structures*, Vol. 106, 2013, pp. 703-715.

[7] Werter N, Breuker RD, "A novel dynamic aeroelastic framework for aeroelastic tailoring and structural optimization," *Composite Structures*, Vol. 158, 2016, pp. 369-386.

[8] Lee DM, Lee I, "Vibration analysis of anisotropic plates with eccentric stiffeners," *Computers & structures*, Vol. 57, No. 1, 1995, pp. 99-105.

[9] Liao CL, Sun YW, "Flutter analysis of stiffened laminated composite plates and shells in supersonic flow," *AIAA journal*, Volo. 31, No. 10, 1993, pp. 1897-1905.

[10] Castro SG, Guimarães TA, Rade DA, Donadon MV, "Flutter of stiffened composite panels considering the stiffener's base as a structural element,". *Composite Structures*, Vol. 140, 2016, pp. 36-43.

[11] Amprikidis M, Cooper J, Rogerson C, Vio G, "On the use of adaptive internal structures for wing shape control in 46th AIAA/ASME/ASCE/AHS/ASC Structures," Structural Dynamics and Materials Conference, 2005.